Supplementary Information for

Design of Mechanically-Robust Naphthalenediimide-based Polymer Additives for High-Performance, Intrinsically-Stretchable Polymer Solar Cells

Chulhee Lim,[†,1] *Sanghun Park,*[†,1] *Dong Jun Kim,*[†,2] *Jin-Woo Lee,*[1] *Jin-Su Park,*[1] *Soodeok Seo,*[1] *Donguk Kim,*[3] *Felix Sunjoo Kim,*[*,3] *Taek-Soo Kim,*[*,2] *and Bumjoon J. Kim*[*,1]

[1]*Department of Chemical and Biomolecular Engineering, Korea Advanced Institute of Science and Technology (KAIST), Daejeon 34141, Republic of Korea*

[2]*Department of Mechanical Engineering, Korea Advanced Institute of Science and Technology (KAIST), Daejeon 34141, Republic of Korea*

[3]*School of Chemical Engineering and Materials Science, Chung-Ang University (CAU), Seoul 06974, Republic of Korea*

[*]Electronic mail: (F. S. Kim) fskim@cau.ac.kr, (T.-S. Kim) tskim1@kaist.ac.kr, (B. J. Kim) bumjoonkim@kaist.ac.kr

Experimental Section

Materials.

Tris(dibenzylideneacetone)dipalladium(0) (Pd_2dba_3) and Tri(o-tolyl)phosphine ($P(o\text{-}tol)_3$) were purchased from the Sigma Aldrich. 4,9-Dibromo-2,7-bis(2-octyldodecyl)benzo[lmn][3,8]phenanthroline-1,3,6,8(2H,7H)-tetraone (NDI2OD-Br) and 5,5'-bis(trimethylstannyl)-2,2'-bithiophene (T2-Sn) were purchased from Derthon Opto electronic Materials Sci. Tech. Co., Ltd. (E)-2,3-Bis(5-(trimethylstannyl)thiophen-2-yl)acrylonitrile (TCVT-Sn) was obtained from 1-materials. Poly[[2,7-bis(2-ethylhexyl)-1,2,3,6,7,8-hexahydro-1,3,6,8-tetraoxobenzo[lmn][3,8]phenanthroline-4,9-diyl]-2,5-thiophenediyl[9,9-bis[3'((N,N-dimethyl)-N-ethylammonium)]-propyl]-9H-fluorene-2,7-diyl]-2,5-thiophenediyl] (PNDIT-F3N-Br) was synthesized by following the previous literature.[1] All the chemicals were purchased from Sigma Aldrich, Alfa Aesar, or Tokyo Chemical Industry (TCI) Co. and used without further purification.

Synthesis

General synthetic procedures for polymer acceptor (P_A): The Pd_2dba_3 (0.02 eq), $P(o\text{-}tol)_3$ (0.08 eq), NDI2OD-Br (1 eq), and T2-Sn (1 eq) for the P(NDI2OD-T2) or TCVT-Sn (1 eq) for the P(NDI2OD-TCVT) were added in the 20 mL vial. The resulting vials were in vacuo for 30 mins and purged with nitrogen. The monomers, catalyst, and ligand were then completely dissolved by injecting organic solvents with or without N,N-dimethylformamide (DMF) (10 v/v%). To obtain P_As of varying molecular weights, the reaction conditions were meticulously manipulated. **Table S1** describes the conditions of synthesis in detail. After the reactions, the crude materials were precipitated in the methanol and purified by the Soxhlet extraction method in the order of methanol, acetone, hexane, and chloroform. The residual solvents were removed by a rotary evaporator. The remaining substances were precipitated again in cold methanol and filtered to obtain each P_A solid.

Characterization. A UV-1800 spectrophotometer was used for obtaining the ultraviolet–visible (UV−Vis) absorption spectra. Cyclic voltammetry was performed using OGF500 model (Origaflex) potentiostat/galvanostat system in a 0.1 M tetrabutylammonium perchlorate solution in anhydrous acetonitrile (degassed with nitrogen), as the supporting electrolyte, at a scan rate of 50 mV s^{-1}. A glassy carbon electrode was used as the working electrode. A platinum wire was used as the counter electrode, and an Ag/AgCl electrode was used as the reference electrode. The redox couple of ferrocene/ferrocenium (Fc/Fc^+) was used as the external standard. The weight-average molecular weight (M_w) and dispersity ($Đ$) of the P_As were determined by size-exclusion chromatography (SEC) analyses with an Agilent GPC 1200 instrument equipped with a refractive index detector, in condition of *ortho*-dichlorobenzene (o-DCB) eluent at 80 °C with polystyrene standards.

Differential scanning calorimetry (DSC) measurement was performed by using DSC 250 (TA instruments). The crystallization and melting transition temperatures (T_c and T_m) and their corresponding enthalpies (ΔH_c and ΔH_m) of the polymers were measured in the 1st cooling and 2nd heating cycles, respectively. The T_c and T_m are the temperatures at which the polymer crystallizes and melts, respectively. The ΔH_c and ΔH_m represent the quantity of thermal energy for the corresponding phase transition during the cooling and heating cycles, respectively.

The grazing incidence wide angle X-ray scattering (GIXS) analysis was conducted in the Pohang Accelerator Laboratory (beamline 3C, Republic of Korea), with incidence angles between 0.12–0.14°. The crystal coherence length (L_c) values of the materials were calculated using Scherrer equation:

$$L_c = \frac{2\pi K}{\Delta_q}$$

(K (shape factor) = 0.9 and Δ_q = full width at half maximum (FWHM) of the scatterings)

The hole and electron mobilities of the pristine and blend films were measured by the space-charge-limited current (SCLC) method using devices with hole-only

(ITO/PEDOT:PSS/active layer/Au) and electron-only device architectures (ITO/zinc oxide (ZnO)/active layer/poly(9,9-bis(3'-(N,N-dimethyl)-N-ethylammoinium-propyl-2,7-fluorene)-alt-2,7-(9,9-dioctylfluorene))dibromide (PFN-Br)/Al). The thicknesses of the blend films were similar to those of the PSC active layers (~110 nm). Current−voltage measurements were performed in the voltage range of 0−1.5 V, and the results were fitted by the Mott-Gurney equation:

$$J_{SCLC} = \frac{9}{8}\varepsilon\varepsilon_0\mu\frac{V^2}{L^3}$$

in which ε is the relative dielectric constant of the pristine and blend constituents, ε_0 is the permittivity of free space (8.85×10^{14} F cm^{-1}), μ is the hole or electron mobility, L is the film thickness, and V is the potential across the device ($V = V_{applied} - V_{bi} - V_r$, where V_{bi} and V_r are the voltage drops induced by the built-in potential and the series resistance, respectively).

Pseudo free-standing tensile measurements were performed following the same sample structures and experimental procedures with the previously reported articles.[2, 3] A high-resolution load-cell was used to measure the load values under strains, and a constant strain rate ($0.8 \times 10–3$ s^{-1}) was applied throughout the measurement. The specimen size for the tensile samples was unified to a 1.7 (for the longer side), 0.5 (for the shorter side), and 0.2 cm (for the middle of the dog-bone shape) length scales. The thicknesses of the pristine films were in a range of 100 – 220 nm.

For the solubility test, the P(NDI2OD-T2) and P(NDI2OD-TCVT) with the M_ws of 250 and 240 kg mol^{-1} were dissolved in chlorobenzene at 100 ℃ for 2 hr. The initial concentrations of the solutions were 20 mg mL^{-1} for the P(NDI2OD-T2) and 30 mg mL^{-1} for the P(NDI2OD-TCVT) due to the fact that all polymers in solutions with much higher concentrations stuck the PTFE filters having 0.45 μm pores. The resulting solutions were then filtered to determine the amount of solutes that were dissolved in the given solvent.

To measure the contact angles of materials, a Phoenix 150 (SEO, Korea) contact angle analyzer was utilized. Using both the contact angles from deionized water (DIW) and glycerol (GY) on thin films, the surface tension of thin films was calculated using the Wu model. The calculation technique is described in detail below:

$$\gamma_{water}(1 + cos\theta_{water}) = \frac{4\gamma_{water}^{d}\gamma^{d}}{4\gamma_{water}^{d} + 4\gamma^{d}} + \frac{4\gamma_{water}^{p}\gamma^{p}}{4\gamma_{water}^{p} + 4\gamma^{p}}$$

$$\gamma_{GC}(1 + cos\theta_{GC}) = \frac{4\gamma_{GC}^{d}\gamma^{d}}{4\gamma_{GC}^{d} + 4\gamma^{d}} + \frac{4\gamma_{GC}^{p}\gamma^{p}}{4\gamma_{GC}^{p} + 4\gamma^{p}}$$

$$\gamma_{total} = \gamma^{d} + \gamma^{p}$$

where γ^{total} is the total surface tension, γ^{d} is the dispersion component, γ^{p} is the polar component, and θ is the contact angle of DIW or GY. Then, based on the surface tensions, the interfacial tension of the materials was calculated using the formula below:

$$\gamma_{12} = \gamma_1 + \gamma_2 - \frac{4\gamma_1^d\gamma_2^d}{\gamma_1^d + \gamma_2^d} - \frac{4\gamma_1^p\gamma_2^p}{\gamma_1^p + \gamma_2^p}$$

where γ_{12} = interfacial tension between two different materials, γ_j (j= 1 or 2) = surface tension of each material, γ_j^d = dispersion component of the surface tension, γ_j^p = polar component of the surface tension.

Polymer Solar Cell (PSC) Fabrication

The PSCs with a normal architecture of indium tin oxide (ITO)/poly(3,4-ethylenedioxythiophene):poly(styrenesulfonate) (PEDOT:PSS) (AI4083) /active layer / poly[[2,7-bis(2-ethylhexyl)-1,2,3,6,7,8-hexahydro-1,3,6,8-tetraoxobenzo[lmn][3,8]phenanthroline-4,9-diyl]-2,5-thiophenediyl[9,9-bis[3'((N,N-dimethyl)-N-ethylammonium)]-propyl]-9H-fluorene-2,7-diyl]-2,5-thiophenediyl] (PNDIT-F3N-Br)/Ag were fabricated following the procedures below. ITO-coated glass substrates were washed with deionized water, acetone, and isopropyl alcohol in a water bath sonicator for 30 min each. After completely drying the residual solvent in a hot oven for 2 hours, the substrates were treated with ozone plasma for 10 min. Then, PEDOT:PSS solution (Clevios, AI4083) was spin-cased onto the prepared substrates at 3500 rpm for 30 s and thermally annealed at 150 ℃ for 15 min. For the PM6-OEG5:(BTP-eC9+P_A) and PM6:(Y7+P_A) systems, the active layer components were dissolved in chlorobenzene at 100 ℃ for an hour with optimized conditions (donor:acceptor = 1:1 (w/w), total concentration = 20 mg mL^{-1}, with 0.5% (v/v) of the 1-chloronaphthalene (1-CN) additive) in a nitrogen-filled glove box. Then, the resultant solutions were maintained at 80 ℃ for 10 minutes before deposited on the ITO/PEDOT:PSS substrate. The active layer solutions were spin-coated on the prepared substrates at 2500 rpm for 60 s. Then, the substrates were thermally annealed at 100 ℃ for 5 min. For the case of PM6:(Y6+P_A) system, the blend constituents were dissolved in chloroform at 50 ℃ for an hour with optimized conditions (donor:acceptor = 1:1.2 (w/w), total concentration = 13.5 mg mL^{-1}, with 0.5% (v/v) of the 1-chloronaphthalene (1-CN) additive) in a nitrogen-filled glove box. Then, the resultant solution was spin-coated on the substrates at 2500 rpm for 60 s, followed by thermal annealing at 90 ℃ for 5 min. P(NDIT-F3N-Br) was dissolved in methanol (1 mg mL^{-1}) at room temperature for an hour, then the P(NDIT-F3N-Br) solution was spin-coated on the ITO/PEDOT:PSS/active layer substrates at 2500 rpm for 30 s. Finally, Ag (120 nm) electrode was deposited under high vacuum (~10^{-6} Torr) in an evaporation chamber. An optical

microscope (Ni-U, Nikon) was used to measure the exact photoactive area of the device (0.04 cm^2). Keithley 2400 SMU instrument was used to measure the PSC efficiency with an Air Mass 1.5 G solar simulator (100 mW cm^{-2}, solar simulator: K201 LAB55, McScience), satisfying the Class AAA, ASTM Standards. K801SK302 of McScience was used as a standard silicon reference cell to calibrate the exact solar intensity.

Intrinsically Stretchable Polymer Solar Cell (IS-PSC) Fabrication

Normal-type IS-PSCs with a device configuration (thermoplastic polyurethane (TPU)/modified PH1000/AI4083/photoactive layers/ PNDIT-F3N-Br/eutectic gallium–indium (EGaIn) were fabricated. The modified PH1000 solution containing dimethyl sulfoxide (DMSO) 5 vol.% (to increase the electrical conductivity of PH1000), polyethylene glycol (PEG) 2 vol.% (to improve mechanical stretchability), (3-glycidyloxypropyl)trimethoxysilane (GOPS) (for thermal crosslinking), and Zonyl fluorosurfactant (Zonyl FS-30) 0.5 vol.% (to enhance the surface wettability) was spin-coated at 1200 rpm for 40 s on the ozone plasma-treated TPU substrate. The TPU-PH1000 substrates were then baked for 20 mins at 100 °C to thermally crosslink the PH1000 layer and prevent its rinsing during the subsequent AI4083 deposition. It is noted that a part of the PH1000 layer was physically protected by the polydimethylsiloxane (PDMS) film for achieving the anode contact. The AI4083 (with PEG 2 vol.%) hole transporting layer was spin-coated at 2500 rpm for 40 s on the PH1000/TPU and treated at 100 °C for 20 min. The photoactive layers were then spin-coated under the same conditions as the fabrication of the PSC on the rigid substrate. On the active layer, 1 mg mL^{-1} of PNDIT-F3N-Br solution in methanol was spin-coated at 2000 rpm for 40 s. Finally, EGaIn liquid metal was sprayed on the PNDIT-F3N-Br film through a deposition mask. The photovoltaic performances of IS-PSC devices were tested by the same instruments with rigid-PSCs, except for the stretching zig. K3100 IQX, McScience Inc. instrument was used to analyze

the external quantum efficiency (EQE) spectra, equipped with a monochromator (Newport) and an optical chopper (MC 2000 Thorlabs).

Supplementary Figures and Tables

Table S1 Detailed conditions for the synthesis of the polymer acceptors (P_As) with different molecular weights (MWs)

P_A	Catalyst	Solvent	Temperature [℃]	Time [h]	End-Capping Agent [mol%]	M_w (Đ) [a] [kg mol^{-1}]
P(NDI2OD-T2)	$Pd_2(dba)_3$/ $P(o\text{-}tol)_3$	Toluene	80	0.5	20	38 (2.2)
		Toluene/ DMF (10 v/v%)	130	12	10	126 (2.5)
					-	218 (2.5)
				72	-	250 (1.9)
P(NDI2OD-TCVT)	$Pd_2(dba)_3$/ $P(o\text{-}tol)_3$	Toluene	80	0.5	20	45 (2.0)
		Toluene	80	1	20	53 (2.1)
		Toluene/ DMF (10 v/v%)	110	12	10	109 (2.3)
					-	182 (2.2)
				72	-	240 (2.3)
		Chlorobenzene/ DMF (10 v/v%)	130	72	-	92.4 (2.3)

* DMF is the abbreviation of the N,N-dimethylformamide.

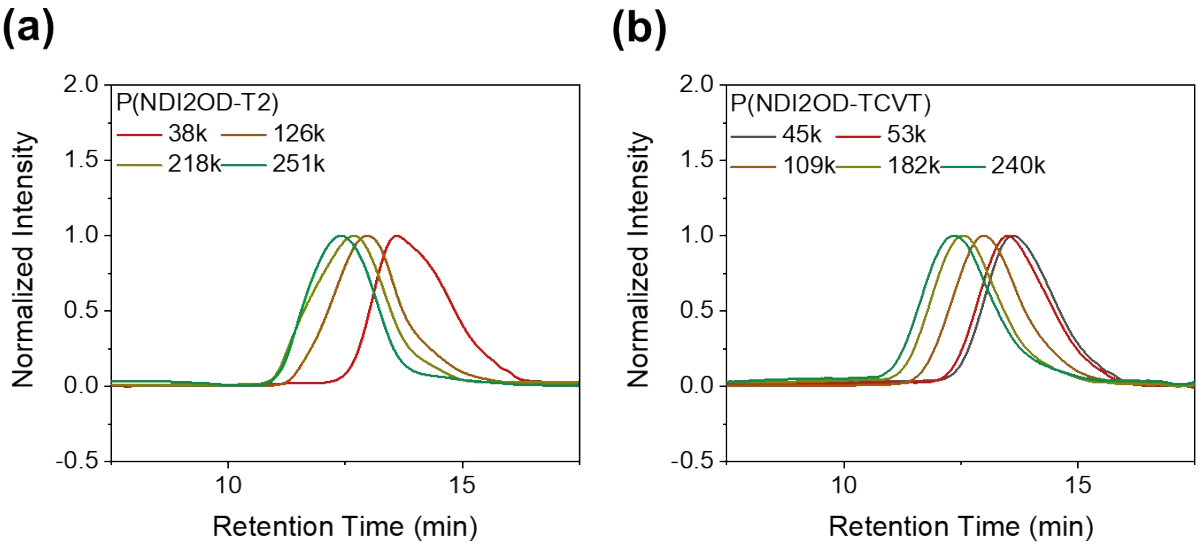

Fig. S1 SEC results for the (a) P(NDI2OD-T2) and (b) P(NDI2OD-TCVT) polymers

Table S2 Solubility of the P_As in chlorobenzene at 100 ℃

P_A	M_w [kg mol^{-1}]	Solubility [mg mL^{-1}]
P(NDI2OD-T2)	250	18.4
P(NDI2OD-TCVT)	240	29.0

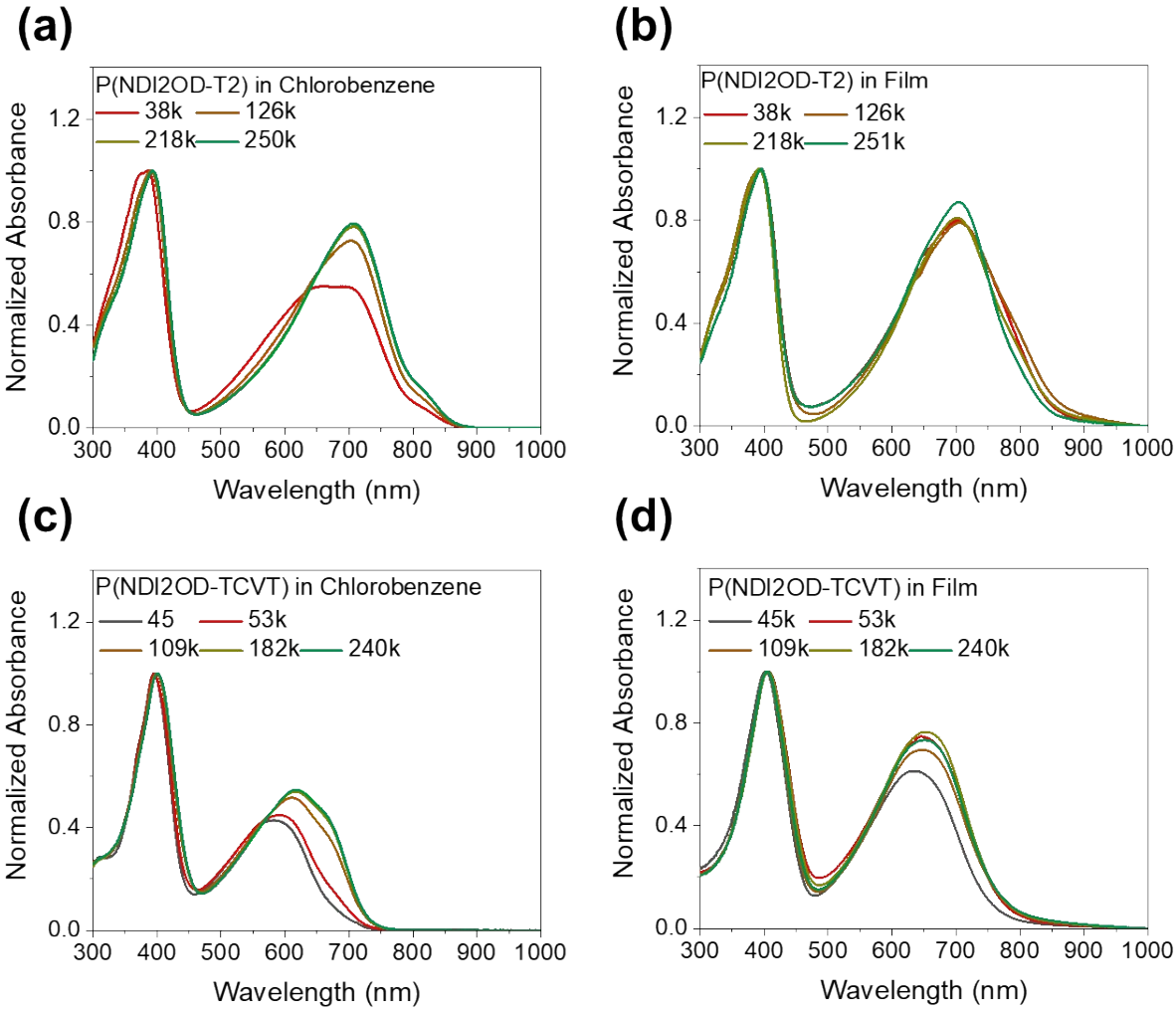

Fig. S2 UV-Vis spectra of the chlorobenzene solutions with the concentration of 0.01 mg mL^{-1} and thin films for the (a), (b) P(NDI2OD-T2) and (c), (d) P(NDI2OD-TCVT) polymers

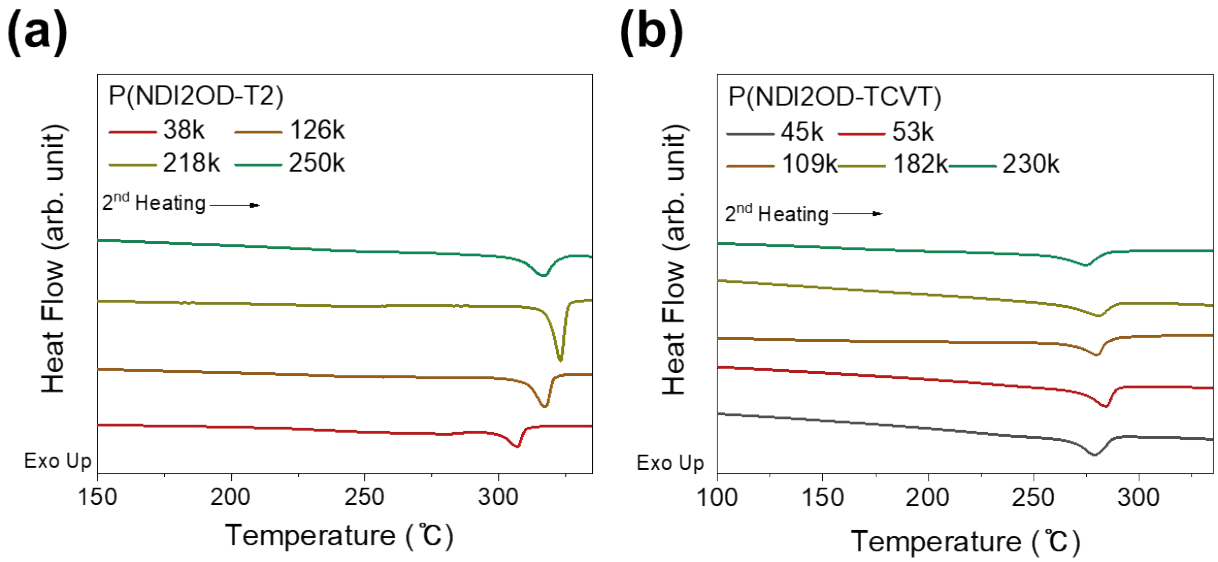

Fig. S3 DSC thermograms of 2nd heating cycles for (a) P(NDI2OD-T2) and (b) P(NDI2OD-TCVT)

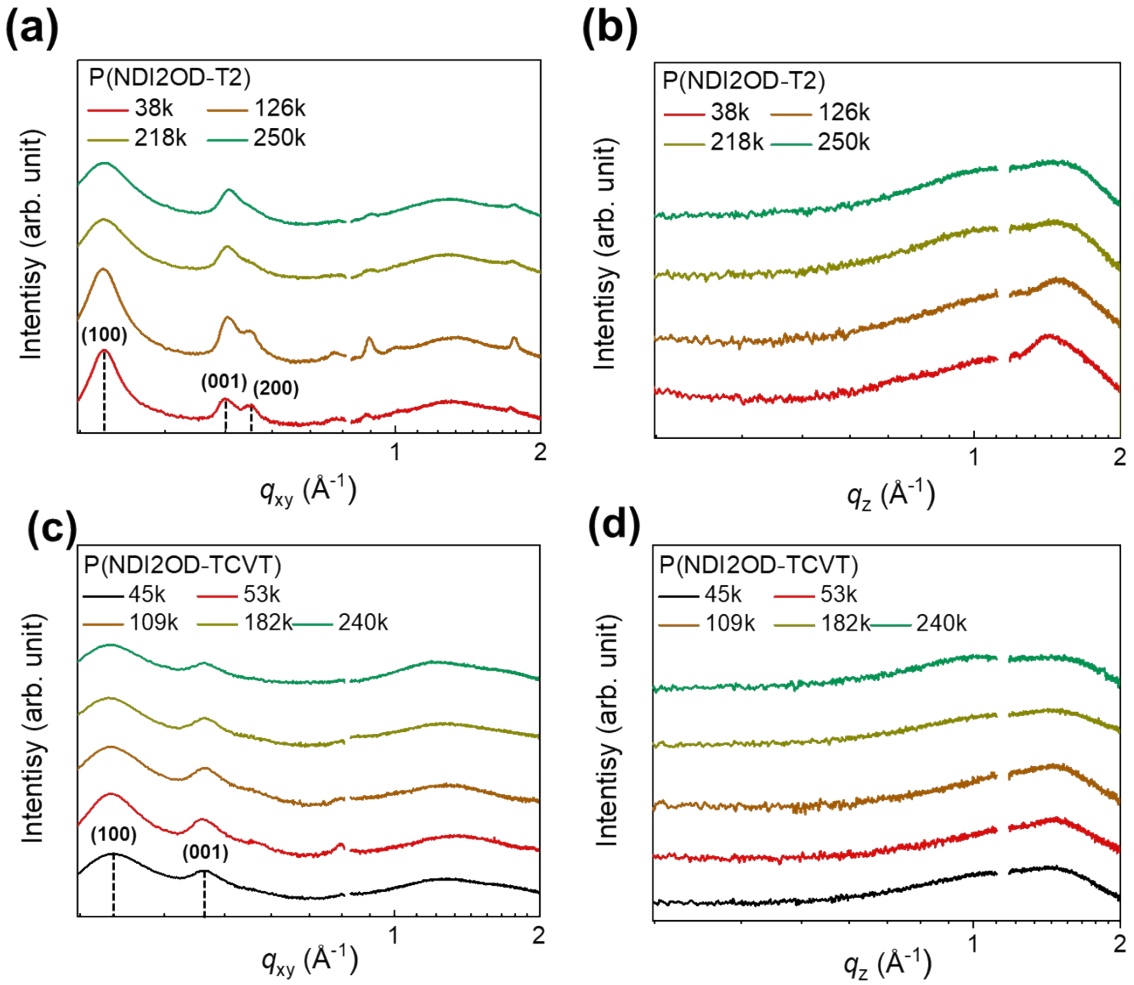

Fig. S4 GIXS profiles in in-plane (IP) and out-of-plane (OOP) direction for the (a), (b) P(NDI2OD-T2) and (c), (d) P(NDI2OD-TCVT) pristine films

Table S3 *d*-spacing and coherence length (L_c) values of the $q_{xy,\ (100)}$ and $q_{xy,\ (001)}$ peaks in the IP direction for the P_As.

P_A	M_w (Đ) [kg mol^{-1}]	$q_{xy,\ (100)}$ [Å^{-1}]	$d_{(100)}$ [Å]	$L_{c,\ (100)}$ [nm]	$q_{xy,\ (010)}$ [Å^{-1}]	$d_{(001)}$ [Å]	$L_{c,\ (001)}$ [nm]
P(NDI2OD-T2)	38 (2.2)	0.25	25.1	24.6	0.45	14.0	18.2
	126 (2.5)			23.6			20.2
	218 (2.5)			14.1			17.1
	251 (1.9)			12.6			16.6
P(NDI2OD-TCVT)	45 (2.0)	0.26	24.2	11.8	0.40	15.7	17.2
	53 (2.1)			13.5			18.2
	109 (2.3)			10.9			17.1
	182 (2.2)			10.3			15.7
	240 (2.3)			9.9			13.8

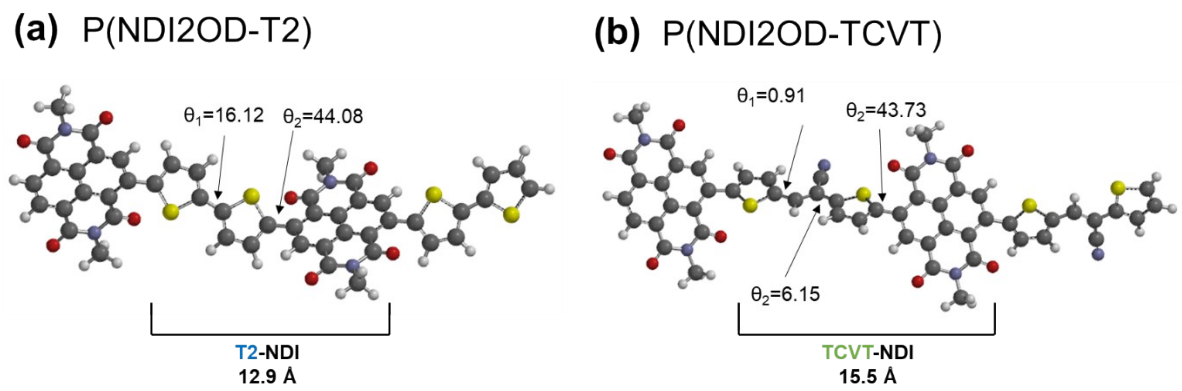

Fig. S5 Dihedral angles and distance between the monomeric units in the (a) P(NDI2OD-T2) and (b) P(NDI2OD-TCVT) polymers from density functional theory (DFT) calculation based on the B3LYP/6-31G* set

Table S4 Elastic moduli, toughness and crack on-set strain (COS) of the pristine thin films for the P_As

P_A	M_w ($Đ$) [kg mol^{-1}]	Elastic modulus [GPa]	COS [%]	Toughness [MJ m^{-3}]
P(NDI2OD-T2)	38 (2.2)	0.17	1.1	0.01
	126 (2.5)	0.80	1.1	0.05
	218 (2.5)	0.65	2.4	0.14
	250 (1.9)	0.73	35.2	7.18
P(NDI2OD-TCVT)	45 (2.0)	0.37	9.5	0.64
	53 (2.1)	0.41	7.9	0.57
	109 (2.3)	0.53	30.1	4.58
	182 (2.2)	0.51	37.1	6.38
	240 (2.3)	0.52	47.1	8.92

Table S5 Photovoltaic performances of rigid PSCs depending on the contents of the P_As in the blends

Blend	V_{oc} (V)	J_{sc} (mA cm^{-2})	FF	PCE$_{max(avg)}$ (%)
PM6-OEG5:BTP-eC9	0.86	24.60	0.73	15.32 (15.20 ± 0.21)
+ P(NDI2OD-T2) 2.5 wt%	0.86	24.77	0.73	15.35 (15.24 ± 0.11)
+ P(NDI2OD-T2) 5 wt%	0.86	25.19	0.72	15.52 (15.44 ± 0.06)
+ P(NDI2OD-T2) 10 wt%	0.86	25.23	0.74	15.94 (15.77 ± 0.12)
+ P(NDI2OD-TCVT) 2.5 wt%	0.86	24.60	0.73	15.45 (15.36 ± 0.07)
+ P(NDI2OD-TCVT) 5 wt%	0.85	25.55	0.72	15.64 (15.60 ± 0.03)
+ P(NDI2OD-TCVT) 10 wt%	0.85	26.36	0.73	16.26 (15.97 ± 0.21)

We note that the results in Table S5 have been added during the revision, which results in a slight difference in the PCE value with those in Table 2.

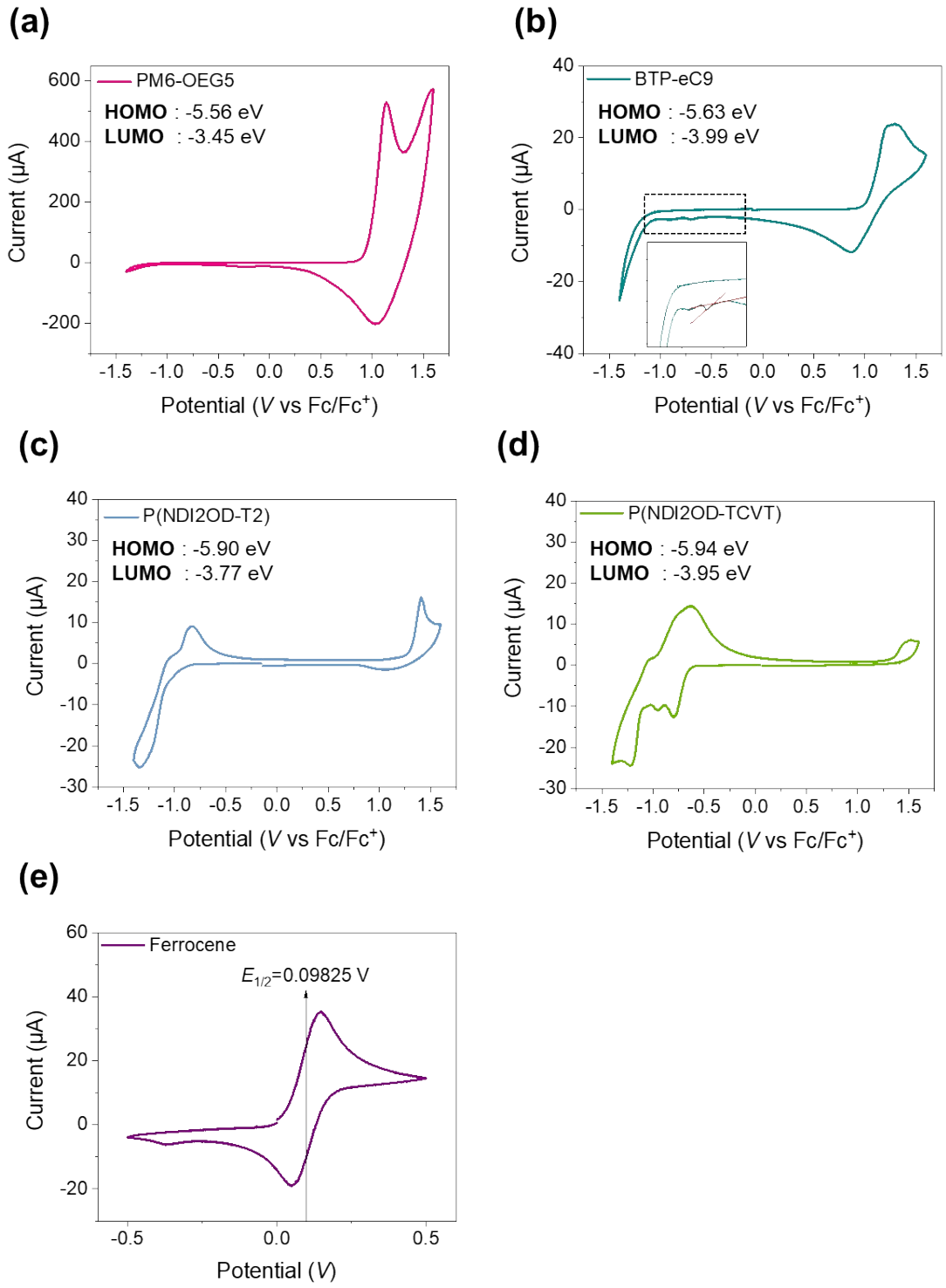

Fig. S6 CV curves measured from neat films of (a) PM6-OEG5, (b) BTP-eC9 and (c) P(NDI2OD-T2) and (d) P(NDI2OD-TCVT), respectively, and from solution of (e) ferrocene in acetonitrile

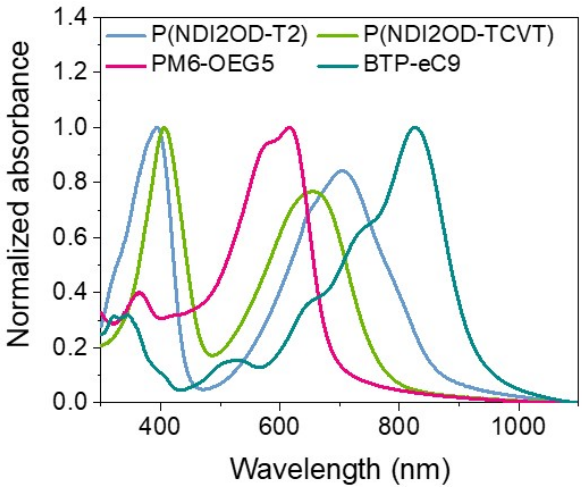

Fig. S7 UV-Vis spectroscopy spectra for the blend constituents of the active layer

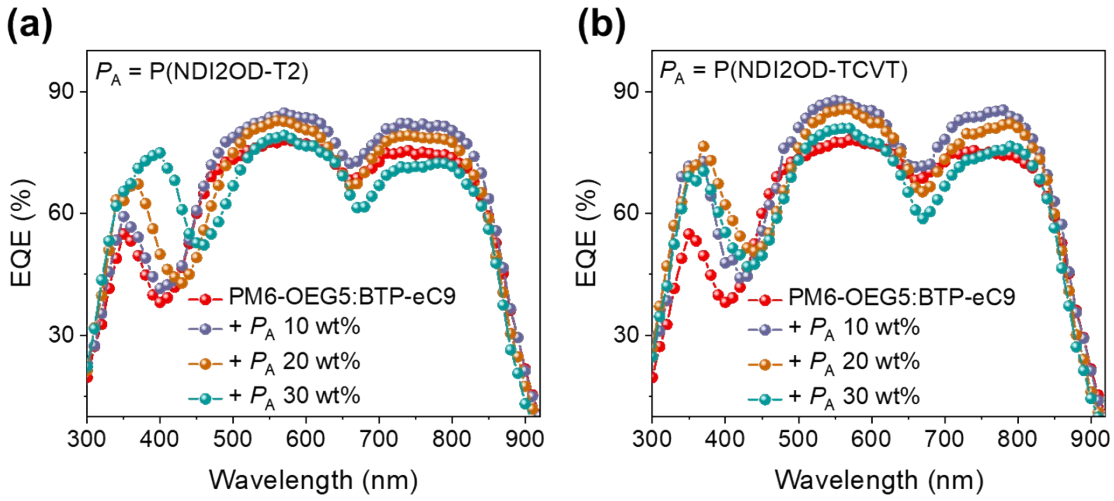

Fig. S8 External quantum efficiency (EQE) spectra of the rigid PSCs based on the binary blend and ternary blends with 10–30 wt% of the (a) P(NDI2OD-T2) and (b) P(NDI2OD-TCVT)

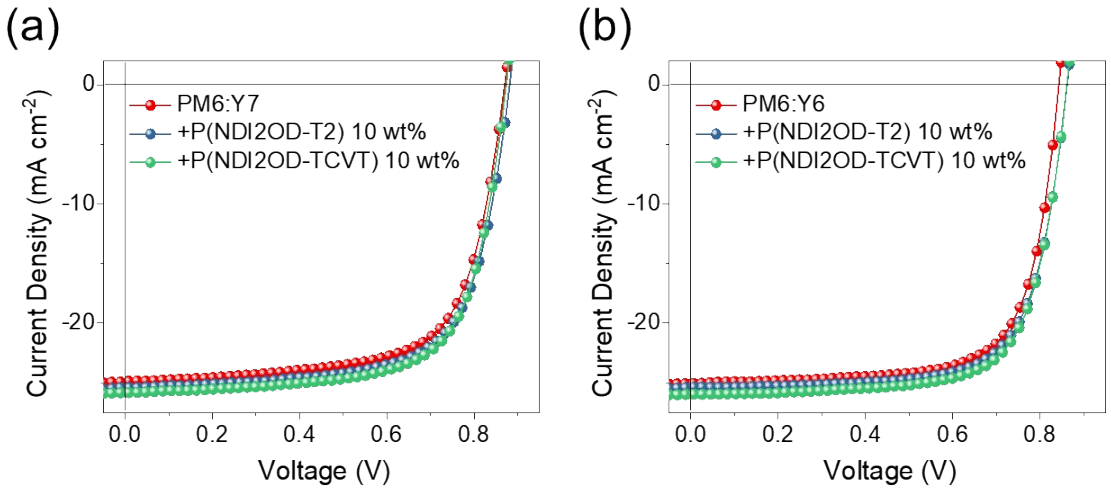

Fig. S9 *J-V* curve of the rigid PSCs with 10 wt% of the P_As as additives in (a) PM6:Y7 and (b) PM6:Y6 blends

Table S6 Photovoltaic performances of rigid PSCs with 10 wt% of the P_As as additives in the PM6:Y7 and PM6:Y6 blends

Blend	V_{oc} (V)	J_{sc} (mA cm^{-2})	FF	PCE$_{max\ (avg)}$ (%)
PM6:Y7	0.87	24.91	0.68	14.87 (14.72 ± 0.08)
+ P(NDI2OD-T2) 10 wt%	0.88	25.44	0.69	15.38 (15.15 ± 0.12)
+ P(NDI2OD-TCVT) 10 wt%	0.87	25.77	0.70	15.63 (15.60 ± 0.08)
PM6:Y6	0.84	24.72	0.71	15.18 (15.03 ± 0.17)
+ P(NDI2OD-T2) 10 wt%	0.86	25.40	0.72	15.66 (15.50 ± 0.15)
+ P(NDI2OD-TCVT) 10 wt%	0.86	25.99	0.72	16.06 (15.87 ± 0.15)

Table S7 Hole and electron mobilities of the blend films

Blend	μ_h [$cm^2\ V^{-1}\ s^{-1}$]	μ_e [$10^{-4}\ cm^2\ V^{-1}\ s^{-1}$]
PM6-OEG5 :BTP-eC9	1.3×10^{-4}	3.0×10^{-4}
+ P(NDI2OD-T2) 10 wt%	1.3×10^{-4}	2.5×10^{-4}
+ P(NDI2OD-T2) 20 wt%	1.2×10^{-4}	2.3×10^{-4}
+ P(NDI2OD-T2) 30 wt%	7.8×10^{-5}	1.0×10^{-4}
+ P(NDI2OD-TCVT) 10 wt%	1.5×10^{-4}	2.7×10^{-4}
+ P(NDI2OD-TCVT) 20 wt%	1.2×10^{-4}	2.5×10^{-4}
+ P(NDI2OD-TCVT) 30 wt%	8.1×10^{-5}	1.7×10^{-4}

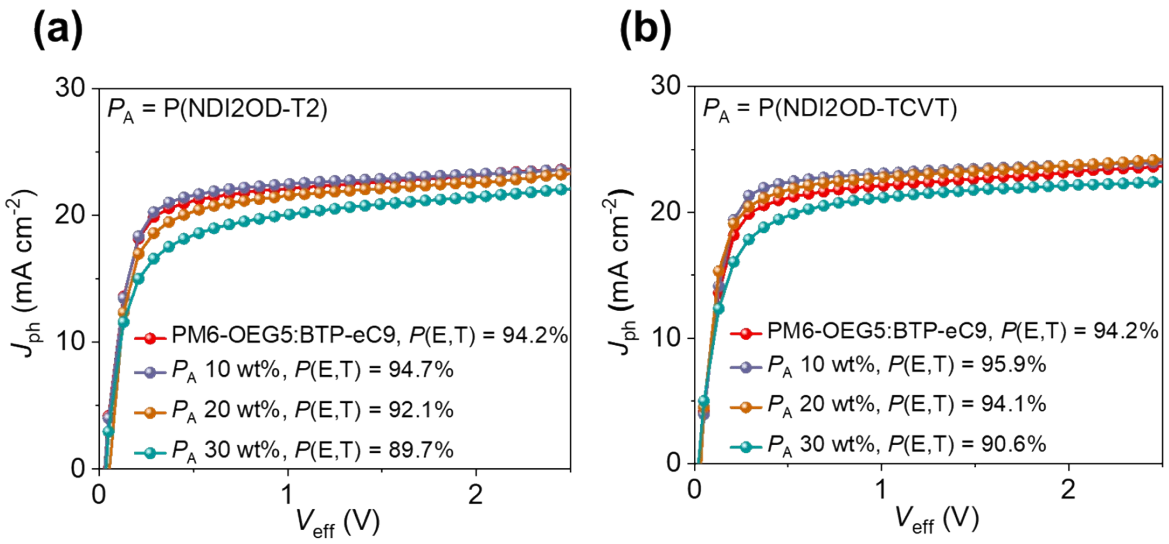

Fig. S10 J_{ph} versus V_{eff} spectra of the IS-PSCs depending on the contents of the (a) P(NDI2OD-T2) and (b) P(NDI2OD-TCVT) polymers

.

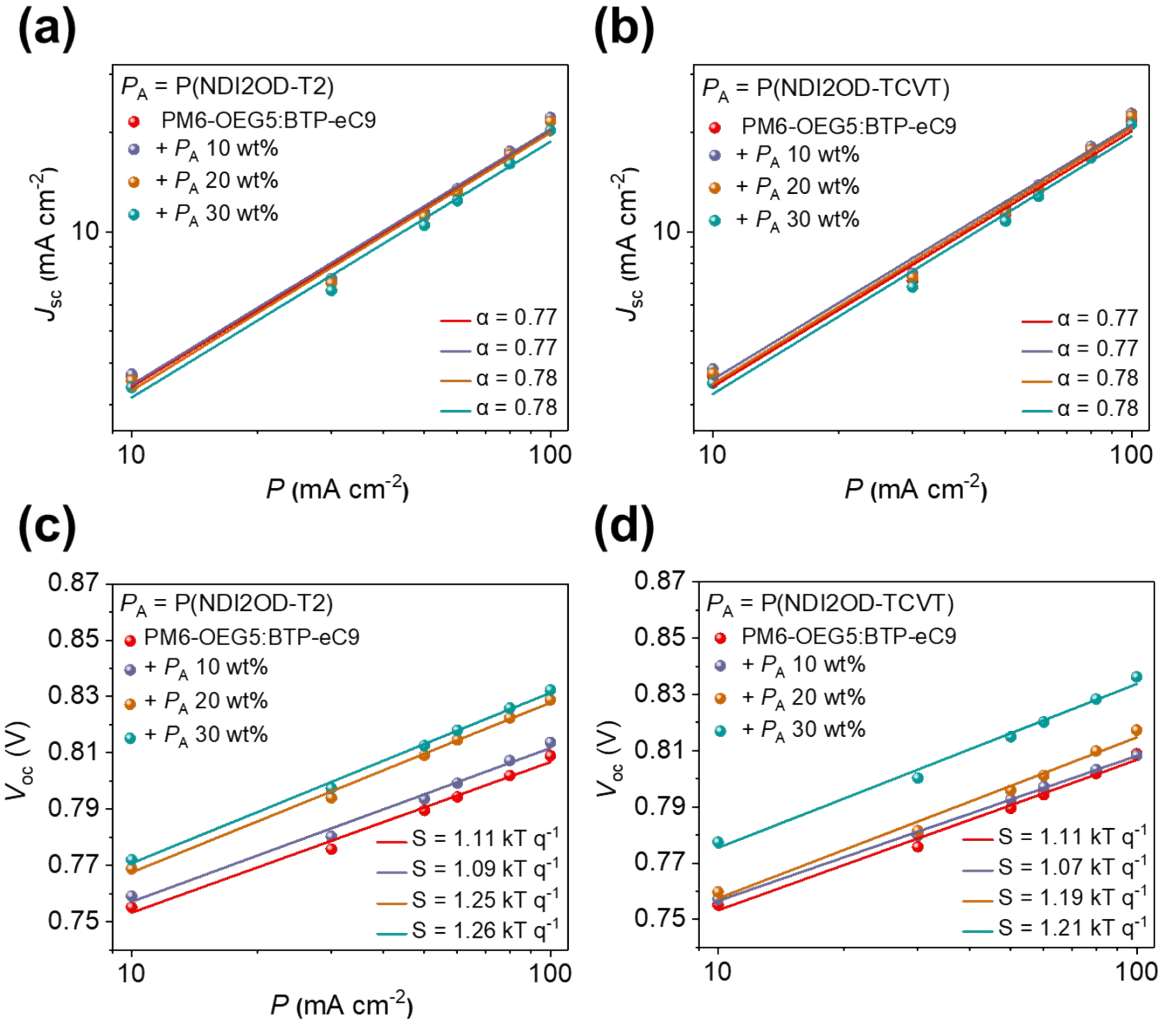

Fig. S11 P versus V_{oc} and J_{sc} spectra of the IS-PSCs depending on the various contents of the (a), (c) P(NDI2OD-T2) and (b), (d) P(NDI2OD-TCVT)

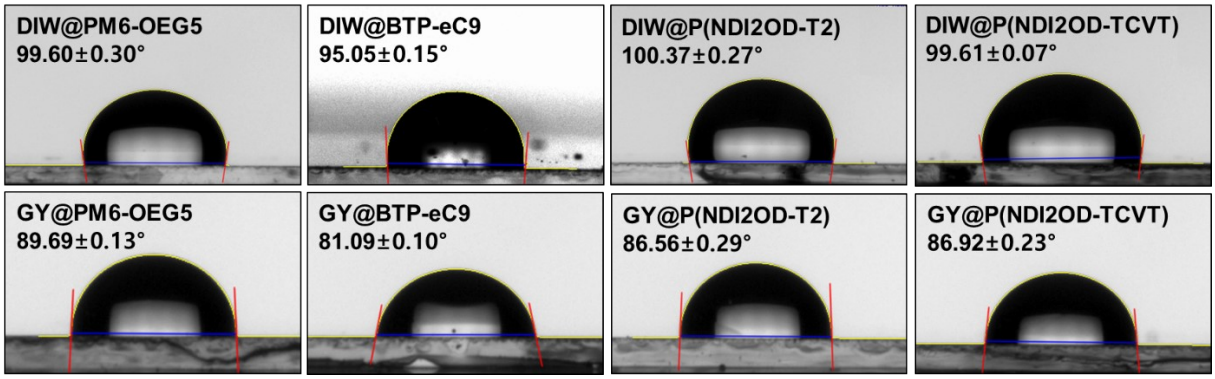

Fig. S12 Contact angles with deionized water (DIW) and glycerol (GY) droplets on the films of each material

Table S8 Contact angles with deionized water (DIW) and glycerol (GY) droplets, surface tensions for the materials, interfacial tensions and wetting coefficients among the materials

Material	θ_{DIW} [°]	θ_{GY} [°]	Surface tension [mN m^{-1}]	$\gamma_{PM6\text{-}OEG5}$ [mN m^{-1}]	$\gamma_{BTP\text{-}eC9}$ [mN m^{-1}]
PM6-OEG5	99.60	89.69	21.3	-	0.94
BTP-eC9	95.05	81.09	26.0	0.94	-
P(NDI2OD-T2)	100.37	89.59	21.5	0.04	0.64
P(NDI2OD-TCVT)	99.61	86.92	23.2	0.53	0.20

To determine the molecular compatibility of the blend components, we measured the contact angles of droplets of deionized water (DIW) and glycerol (GY) on their respective thin films (**Fig. S12**). Using the Wu model, the surface tension and interfacial tension (γ) between the materials were estimated (**Table S8**).[4] As a result, the γ with BTP-eC9 ($\gamma_{BTP\text{-}eC9}$) for each P_A was calculated to be 0.64 for P(NDI2OD-T2), and 0.20 for P(NDI2OD-TCVT), respectively. Thus, we anticipated that P(NDI2OD-TCVT) would interact with SMA more favorably than P(NDI2OD-T2), bridging different SMA domains in the active layer more effectively.

Reference

1. Z. Wu, C. Sun, S. Dong, X.-F. Jiang, S. Wu, H. Wu, H.-L. Yip, F. Huang and Y. Cao, *J. Am. Chem. Soc.*, 2016, **138**, 2004-2013.
2. J.-H. Kim, A. Nizami, Y. Hwangbo, B. Jang, H.-J. Lee, C.-S. Woo, S. Hyun and T.-S. Kim, *Nat. Commun.*, 2013, **4**, 2520.
3. J. Choi, W. Kim, D. Kim, S. Kim, J. Chae, S. Q. Choi, F. S. Kim, T.-S. Kim and B. J. Kim, *Chem. Mater.*, 2019, **31**, 3163-3173.
4. K.-H. Kim, H. Kang, H. J. Kim, P. S. Kim, S. C. Yoon and B. J. Kim, *Chem. Mater.*, 2012, **24**, 2373-2381.